

1 **Evidence against a general positive eddy feedback in atmospheric blocking**

2
3 **Lei Wang^{1,2} and Zhiming Kuang^{1,2}**

4 ¹ Department of Earth and Planetary Sciences, Harvard University, Cambridge, MA, USA.

5 ² John A. Paulson School of Engineering and Applied Sciences, Harvard University, Cambridge,
6 MA, USA.

7
8 Corresponding author: Lei Wang (leiwang@g.harvard.edu)

9
10 **Key Points:**

- 11 • Atmospheric blocks can be simulated in a zonally symmetric two-layer quasi-geostrophic
12 model without topography.
- 13 • Randomly selected synoptic eddies do not reinforce the blocks through a positive
14 feedback, challenging the eddy straining mechanism.
- 15 • The second-order induced flow, previously used to support the general eddy feedback
16 idea, is sensitive to the location of the wave maker.

17 **Abstract**

18 The eddy straining mechanism of Shutts (1983; S83) has long been considered a main process
19 for explaining the maintenance of atmospheric blocking. As hypothesized in S83, incoming
20 synoptic eddies experience a meridional straining effect when approaching a split jetstream, and
21 as a result, enhanced PV fluxes reinforce the block. A two-layer QG model is adopted here as a
22 minimal model to conduct mechanism-denial experiments. While transient eddies' forcing is
23 clearly critical to the formation and maintenance of a block, using a large ensemble, the authors
24 demonstrate that the straining of generic eddies does not maintain blocks, thus challenge the idea
25 of eddy straining serving as a positive feedback for the blocks. These results indicate that
26 specific configurations of the eddy field are required for the maintenance stage. The authors also
27 remark on the main supporting evidence in S83: the second-order induced flow is sensitive to the
28 location of the wavemaker.

29

30 **Plain Language Summary**

31 Atmospheric blocking is an important process for both weather and climate. The eddy straining
32 mechanism of Shutts (1983) has been considered as the foundation to understanding the
33 maintenance of blocks, which is consistent with the observation that strong wave breaking is
34 always concurrent with strong blocks. However, the authors here use a large-ensemble of a two-
35 layer quasi-geostrophic model to assess whether such a correlation is due to a causal relationship
36 between the straining of generic eddies by the block and block enhancement, as proposed by
37 Shutts (1983). Surprisingly, the authors demonstrate that the generic effects from straining eddies
38 is insignificant to the maintenance of the blocking pattern. The authors also note an important
39 issue with the experimental design and the physical relevance of the weakly nonlinear
40 simulations in Shutts (1983). Therefore, the authors challenge the existence of a generic
41 mechanism of positive eddy feedback, and attribute the blocks' actual maintenance to the
42 specific initial condition of pre-existing eddies, which intrinsically depends on chance.

43 **1 Introduction**

44 Atmospheric blocking is an important phenomenon characterized by a quasi-stationary
45 and large-scale meridional dipole flow fields in the mid-latitude atmosphere. A common feature
46 across most blocking types is a meridional dipole in the anomaly field of PV or geopotential
47 height. Once a block has been established, such a dipole structure can persist for more than the
48 synoptic timescale, exerting impacts on local weather with significant societal implications.

49 During a blocking episode, synoptic weather systems propagate from upstream and can
50 interact with the blocking dipole (Berggren et al., 1949). Such transient waves' forcing is critical
51 for the maintenance of a block (Holopainen & Fortelius, 1987; Woollings et al., 2018). This
52 paper is focused on the role of eddies during the maintenance stage of blocks, by addressing an
53 open question regarding whether generic incoming eddies can reinforce a block as a positive
54 feedback.

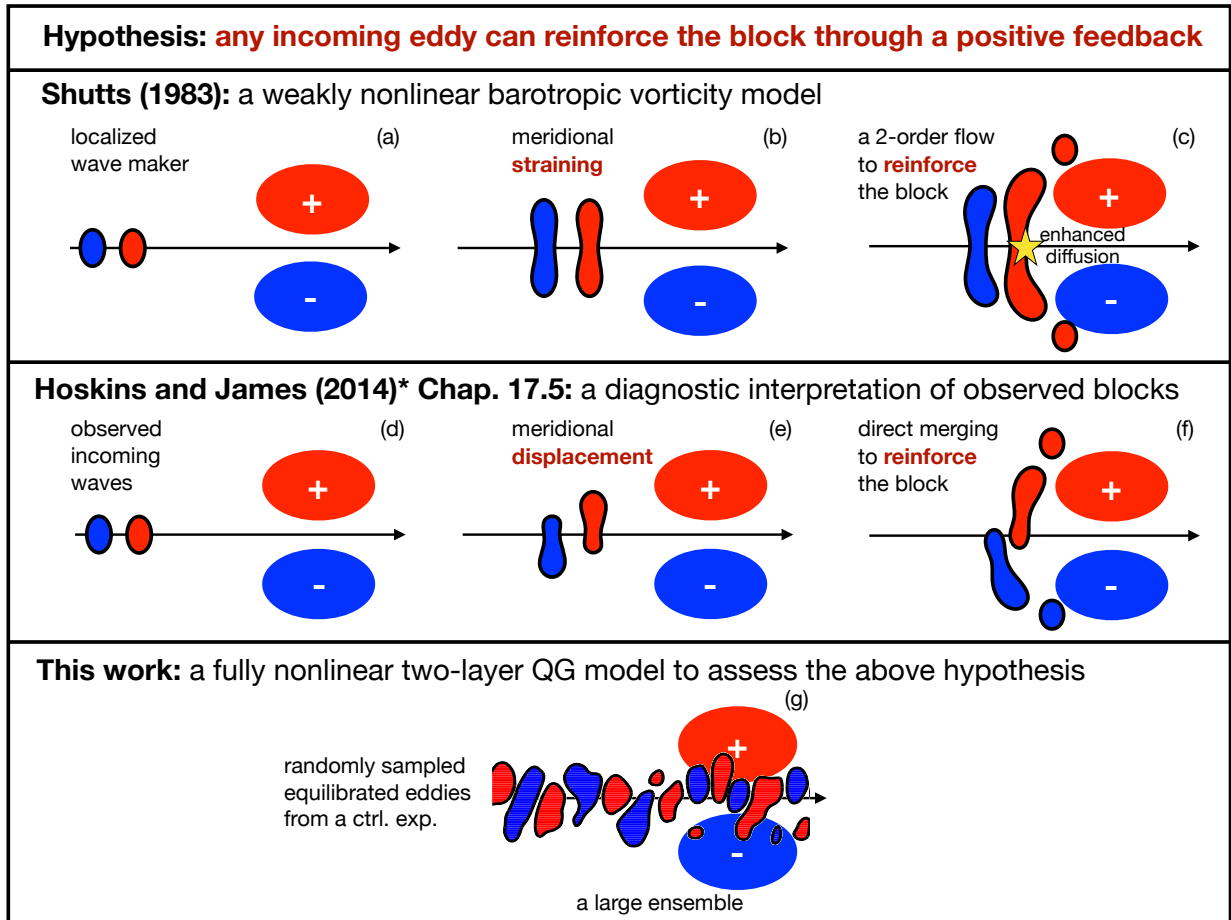
55 A seminal paper by Shutts (1983) (S83) proposed a mechanism that, as synoptic eddies
56 approach a block, they will be strained meridionally, and the enhanced diffusion near the point of
57 jet splitting can drive a meridionally asymmetric second-order flow. Importantly, using a weakly
58 nonlinear model, S83 demonstrates that the numerical solution of the second-order flow has an
59 in-phase structure that reinforces the existing block's amplitude. At the same time, observational
60 evidence suggests that, during a mature block, warm air can move poleward and eventually cut
61 off anticyclonically from incoming waves to directly merge with the blocking anticyclones, and
62 the opposite is true for cold air to merge with the blocking cyclones. This is termed the selective
63 absorption mechanism (Yamazaki & Itoh, 2012) (YI12) and the essential physical process is
64 schematically described in Section 17.5 of a textbook by Hoskins and James (2014) (HJ14). Both
65 mechanisms are schematically summarized in Fig. 1a-f. Note that both mechanisms assume the
66 initial incoming eddies are meridionally symmetric, which is consistent with the observations of
67 mid-latitude eddies. In this paper, we will not address studies using the modon solution (e.g.
68 Haines & Marshall, 1987) because of the strong instability of a modon and the sensitivity to
69 domain configurations (Arai & Mukougawa, 2002).

70 The observational evidence is indeed compelling that synoptic eddies strain and shift
71 meridionally during a mature block. However, such evidence does not necessarily imply that any
72 incoming eddies can systematically reinforce the block as a generic positive feedback
73 mechanism, as hypothesized in S83, which imposed no restrictions on the incoming eddies. An
74 alternative interpretation to a generic positive feedback would be that only under certain
75 conditions of the pre-existing synoptic eddies can a dipole structure in eddy forcing be developed
76 through nonlinear eddy-eddy interactions to reinforce the block. In this case, eddy straining,
77 meridional shifts, and wave breaking would occur but there is no generic positive feedback;
78 whether a block persists is determined by conditions of the pre-existing synoptic eddies.

79 To rule out the sensitivity to the initial conditions of pre-existing synoptic eddies, we aim
80 to test whether any substantial reinforcing effect is present and identifiable when we randomly
81 sample initial conditions from equilibrated baroclinic eddy fields. We adopt a minimal model for
82 tackling this issue: a two-layer quasi-geostrophic model, which is fully nonlinear and
83 baroclinically unstable without the need of a wavemaker. In the next section, we will illustrate
84 that blocking maintenance cannot be supported by randomly selected equilibrated flow field,
85 casting doubt on the existence of the positive eddy feedback hypothesized in S83.

86

87
88
89



90
91
92

Figure 1. A schematic diagram of three different approaches for testing the hypothesis whether generic eddies can reinforce the block as a positive feedback.

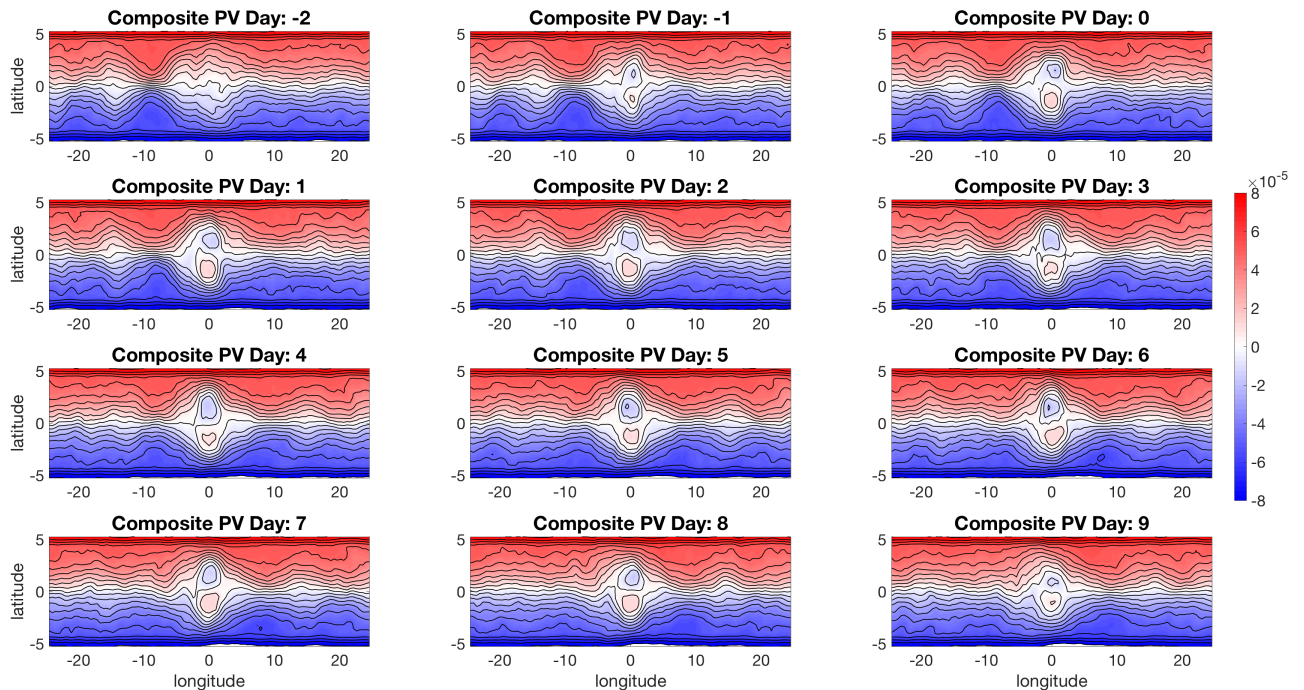
93 2 A Mechanism-Denial Study

94 2.1 A two-layer quasi-geostrophic model

95 A main issue with the barotropic model used in prior studies is that incoming waves can
 96 only be prescribed with a wavemaker. A two-layer QG model is a minimal model that can
 97 intrinsically generate synoptic eddies that are equilibrated across the domain. A two-layer model
 98 has been used to study blocks (Vautard et al., 1988; K. Haines & Holland, 1998; Luo, 2000). To
 99 extract the full pattern of a mature block, we integrate a two-layer QG model for 100000 days
 100 and take the last 90000 days for composite analysis. See Appendix A for more details on the
 101 model.

102 We define blocking based on local finite-amplitude wave activity (LWA) (Huang &
 103 Nakamura, 2016), which bears a clear physical meaning: large values of wave activity
 104 straightforwardly correspond to an overturn of PV contours in both the north and south sides of a
 105 certain latitude. With a threshold of 1.5 standard deviation of LWA variability, 351 blocks that
 106 last at least 10 days are identified. These blocks will be used for the composite. The exactly
 107 number of blocks would of course vary with different threshold values, but salient features of the
 108 blocks remain the same for strong and persistent blocks. Fig. 2 demonstrates the evolution of
 109 total PV fields in the upper layer of the QG model from the composite.

110



111

112 **Figure 2.** Composite blocks in a two-layer QG model. Evolution of the upper layer PV from two
 113 days prior to the onset of the block to day 9. The contour interval is $0.2 \times 10^{-5} \text{ s}^{-1}$.

114

115 **2.2 Evolution of the eddy PV flux divergence**

116 The ensemble-mean evolution of the barotropic eddy PV can be described as:

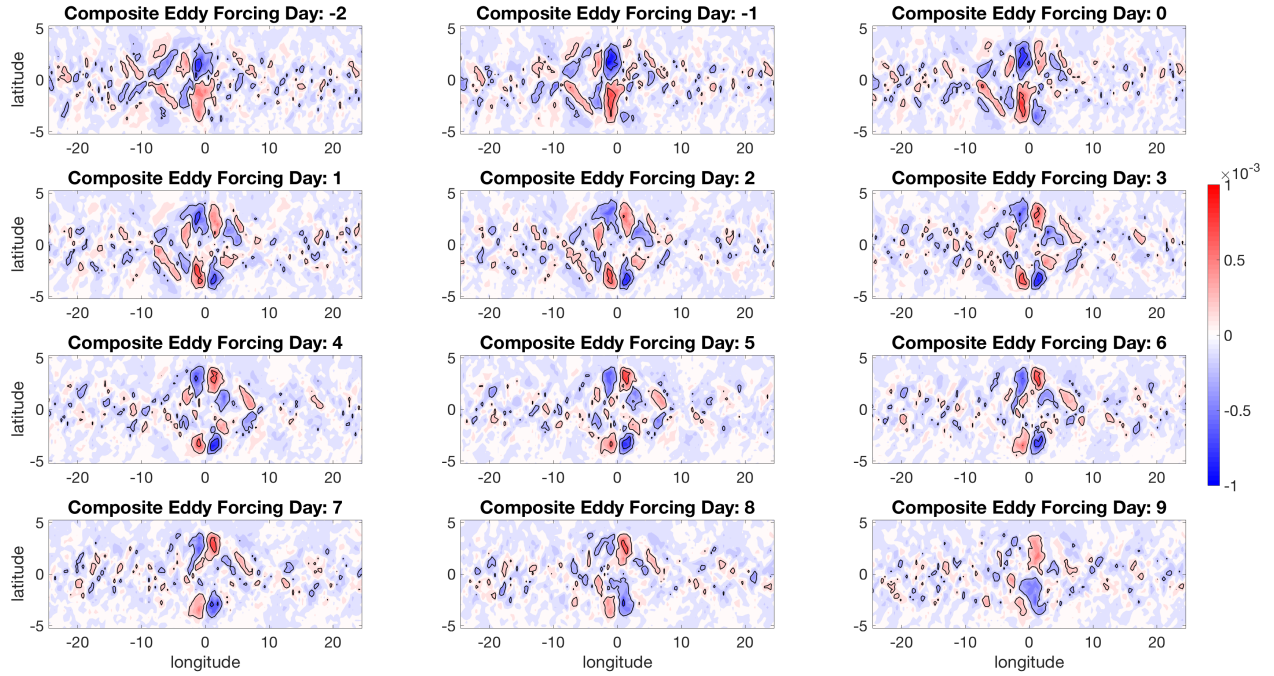
117
$$\frac{\partial [q_b']}{\partial t} + J([\psi_b], [q_b]) = -\nabla \cdot [\mathbf{v}_b' q_b'] + [D] \quad (1)$$

118 where $[\cdot]$ denotes ensemble average, subscript b denotes barotropic component, and D
 119 represents dissipation (associated with 6th-order hyper-viscosity) and Ekman damping. During
 120 the mature stage of blocks in this model, on the leading order, the mean flow advection of block
 121 is balanced by the planetary vorticity advection and self-advection by the block (not shown), i.e.
 122 $J([\psi_b], [q_b]) \sim 0$, therefore the eddy PV flux divergence $-\nabla \cdot [\mathbf{v}'q']$ (hereafter as eddy forcing) is
 123 the dominant driving force for the ensemble-mean evolution of the eddy PV. As shown in Fig. 3,
 124 the ensemble-mean eddy forcing shows a consistent dipole structure at the beginning stage of the
 125 composite (even two days before blocking onsets), and gradually switches to a negative phase
 126 after day 8 which would eventually damp the block toward the end of the block lifecycle. Such
 127 evolution suggests that transient eddies are responsible for the full evolution of the block.

128 However, the importance of transient eddies does not necessarily imply the existence of a
 129 general positive eddy feedback as a result of either straining (as described by S83) or meridional
 130 displacements (as described by YI12 and HJ14) of a generic eddy field. It remains possible that,
 131 by compositing on strong and persistent blocks, we have selected eddy fields with specific
 132 configurations and those specific configurations, instead of a general eddy feedback, are the key
 133 to the resulting eddy forcing that maintains the block. Next we turn to simulations using
 134 randomly selected eddy fields in order to evaluate the existence of a general eddy feedback.

135

136



137

138 **Figure 3.** Composite Eddy PV flux divergence $-\nabla \cdot [\mathbf{v}'q']$ in a two-layer QG model,
 139 corresponding to the PV evolution in Fig. 2. The contour interval is $4 \times 10^{-4} \text{ s}^{-2}$.

140

141

142 **2.3 A large-ensemble simulations to assess the hypothesis**

143 To answer the question proposed in the last section, we now assess whether a randomly
 144 selected PV field can reinforce a block as predicted in S83. Based on the composite, we take the
 145 blocking pattern q'_{block} , which is defined as the anomaly field (departure from zonal-mean) at
 146 day 7 of the composite block, and add it to three thousands randomly selected PV fields q_i from
 147 the control run for both layers, such that the ensemble mean of the flow field satisfies:

$$148 \quad [q_i + q'_{block}] = \bar{q} + q'_{block} \quad (2)$$

149 where \bar{q} refers to the climatological basic state of the control run. In other words, the procedure
 150 guarantees that the ensemble-mean basic state equals to the model control run's basic state plus
 151 the mature blocking anomaly.

152 Under this experiment design, we stress that, in the ensemble-mean sense, while the
 153 contribution from deformed eddies (i.e. strained eddies) is well represented as it is ubiquitous in
 154 a turbulence flow, no contribution is allowed from the specific pre-existing eddies associated
 155 with blocking, because the random selection of the PV fields as initial conditions does not favor
 156 any specific configurations of such eddies.

157 The resulting ensemble-mean block retains its dipole structure for only 3 days (See
 158 Figure S1). This is an indication that the transient eddies, when they are randomly sampled, do
 159 not contribute substantially to the maintenance of the block. However, it is still possible that such
 160 a lack of reinforcement could due to the rapid (~ 3 days) collapse of the block. Therefore, we add
 161 a time-invariant corrector of PV in both layers to ensure that a mature block pattern is robustly
 162 maintained throughout the calculation. The time-invariant corrector is based on the negative
 163 tendency of the ensemble-mean drift in day 1. With this corrector, the block structure is well
 164 retained up to day 12 (See Figure S2).

165 A striking result is that, in Fig. 4, the ensemble-mean eddy forcing is almost zero
 166 everywhere. If the transient eddies are reinforcing the block as a positive feedback, we would
 167 expect the results, at least its order of magnitude, to be consistent with that in Fig. 3 from the
 168 composite. This result suggests that it is the specific initial condition that leads to the block
 169 maintenance, instead of a positive feedback as a result of eddy straining and meridional shifts by
 170 the block.

171

172

173

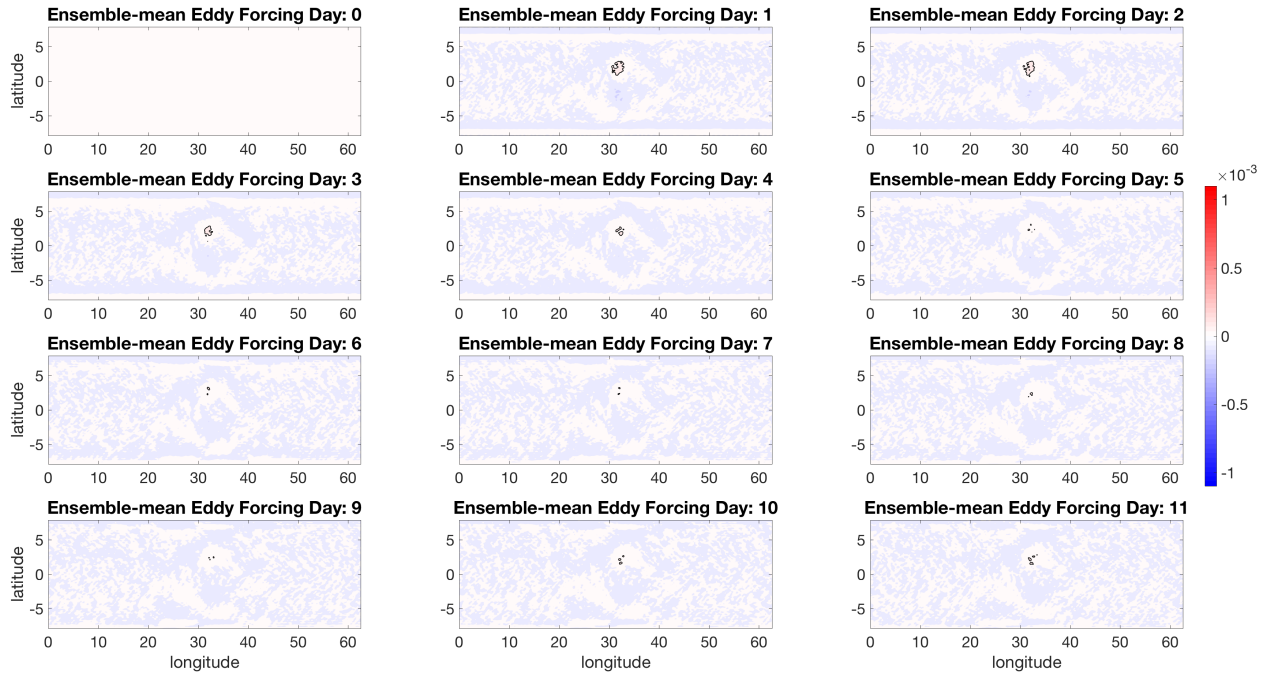
174

175

176

177

178



179

180 **Figure 4.** The ensemble-mean eddy PV flux divergence $-\nabla \cdot [\mathbf{v}'q']$ in a large-ensemble of a two-
 181 layer QG model. Note the same contour levels to that in Fig. 3.

182

183

184 **3 Re-examining the results in Shutts (1983)**

185 The fully nonlinear result in the last section is in contradiction to the positive eddy
 186 feedback hypothesis proposed by S83. The main supporting evidence in S83 was a weakly
 187 nonlinear barotropic model with a localized wavemaker. In this section, following the
 188 methodology of S83, we perform a weakly nonlinear calculation of the barotropic component of
 189 the two-layer QG model to seek the second-order induced flow. See Appendix B for details of
 190 the model. The zero-th order flow is based on the mature stage of the composite barotropic PV
 191 q_{block} from the two-layer model.

192 In Case 1, as shown in Figs. 5(a)(c), when the wave maker is placed immediately
 193 upstream of the block, the second-order induced flow shows a pattern consistent with the
 194 blocking dipole suggesting that reinforcement is possible, which is qualitatively consistent with
 195 S83.

196 However, in Case 2, as shown in Figs. 5(b)(d), when the wavemaker is placed far
 197 upstream, the second-order induced flow shows an opposite pattern over the block region
 198 suggesting that reinforcement is not identifiable. This is in contraction with S83, and
 199 demonstrates a strong sensitivity of the results to the location of the wavemaker. Such sensitivity
 200 to the location of the wave maker casts doubt on the interpretation of the results in S83. In fact, a
 201 similar sensitivity has been reported earlier for a barotropic model with realistic flow pattern
 202 (Maeda et al., 2000).

203 As hypothesized by S83, as a result of enhanced enstrophy production at the point of jet
 204 splitting, one may expect an enhanced diffusion to induce a second-order flow, whose spatial
 205 structure, according the calculations done in S83, is to reinforce the block. Note that such
 206 enhanced diffusion would exist even without a block as the eddies disperse zonally and
 207 meridionally, as long as there is a background PV gradient (such as the planetary vorticity
 208 gradient), see the results in Case 3 in Figs. 5(e)(g). Therefore, with the approach in S83, a
 209 technical challenge is to exclude the influence from the wave maker itself, which isn't
 210 straightforward for a barotropic model that has to place a wave maker somewhere.

211 To eliminate the influence from the location of the wave maker, we conduct an ensemble
 212 of weakly nonlinear calculations. For each member, we place the wave maker at a different
 213 longitude. The difference in the longitude between adjacent members is $1.25\pi L_d$, where L_d
 214 denotes the radius of deformation in the QG model. With 16 members, the ensemble covers the
 215 entire zonal extent. Because of cancelations between simulations with wave makers close to the
 216 block and far upstream of the block, the ensemble-mean second-order induced flow (Figs.
 217 5(f)(h)) is one order smaller than that in Cases 1 and 2. The ensemble-mean second-order
 218 induced flow shows a quadruple structure with little projection onto the blocking dipole.

219

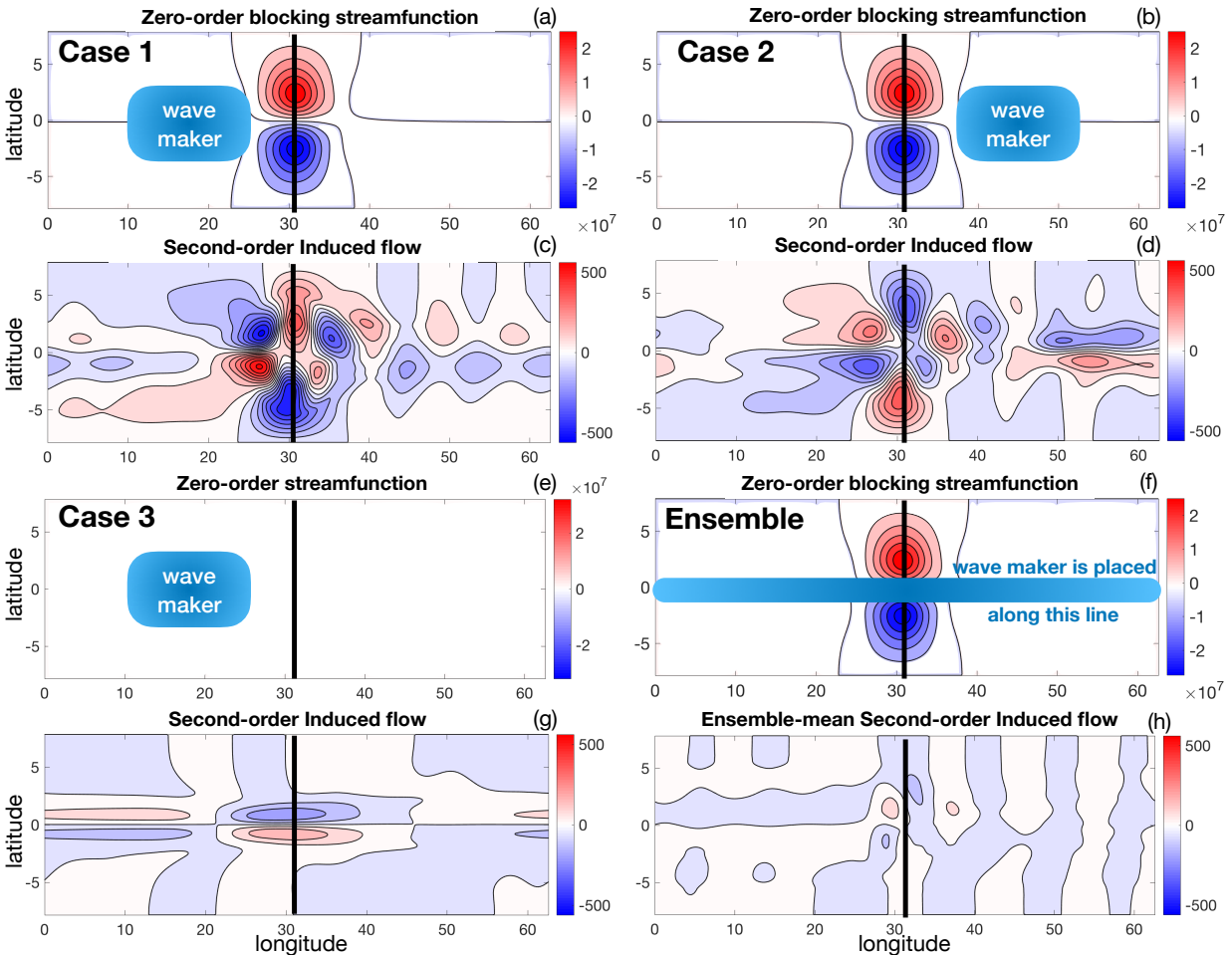
220

221

222

223

224



225

226 **Figure 5** (a)(c) The zero-order blocking streamfunction and the second-order induced flow for
 227 Case 1 where the wave maker is close upstream of the block. (b)(d) Similar to Case 1, but the
 228 wave maker is placed far upstream of the block. (e)(g) Similar to Case 1, but the zero-order
 229 streamfunction does not contain a block. (f)(h) Similar to Case 1, but is a 16-member ensemble
 230 average where for each member the wave maker is placed at a different longitude along the blue
 231 line marked in (f). In (a)(b)(e)(f), the contour interval for the zero-order streamfunction is 4×10^6
 232 $\text{m}^2 \text{s}^{-1}$ and in (c)(d)(g)(h) the contour interval for the second-order induced flow is $7 \text{m}^2 \text{s}^{-1}$.

233

234

235 **4 Discussions**

236 The discrepancy between the ensemble of the weakly nonlinear calculations in Section 3
237 and the fully nonlinear simulations in Section 2 presumably arises from the several assumptions
238 made in the weakly nonlinear calculations in S83. These assumptions include:

- 239 (1). Finite-amplitude synoptic eddies can be qualitatively treated as small-amplitude waves;
- 240 (2). The baroclinic-barotropic interaction is not essential;
- 241 (3). In the presence of a block, the horizontal distribution of the synoptic eddy activity can be
242 simplified as a localized wavemaker.

243 Beyond these assumptions made, why is the enhanced diffusion not working as expected
244 in S83 to provide the eddy forcing that reinforces the block? It is true that a high enstrophy
245 production must lead to an enhanced diffusion as argued in S83, but the location of such
246 enhancement does not coincide with the jet split region. Note that wavemaker *per se* generates
247 enstrophy. In fact, in S83's Fig. 4(d), when the wavemaker is placed away from the jet splitting
248 region, no enhanced enstrophy can be identified at the jet splitting region. Instead, two local
249 maxima occur near the two jet branches of the block. Lastly, why does the zonal convergence of
250 wave activity not maintain the mature block? We speculate that as synoptic eddies strain, they
251 can propagate along the two jet branches and disperse away meridionally, preventing the local
252 wave activity associated with the strained eddies from building-up. These processes will be
253 investigated in future work.

254

255 **5 Conclusions**

256 Despite the evidence that a sequence of events, including eddy straining, meridional
257 shifts, and wave breaking, are observed to be concurrent with the mature stage of blocks, we
258 show that synoptic eddies do not reinforce the block as a general positive feedback mechanism
259 when the initial conditions are randomly sampled.

260 Our results illustrate the important role of the initial conditions of the pre-existing eddies
261 in giving rise to the lifecycle of blocks. Specific configurations of pre-existing eddies must be
262 instrumental for blocking maintenance, which, when satisfied, provide conducive condition for
263 meridional displacement as well as the subsequent wave breaking to occur, which is the reason
264 of the concurrency in the observations. Detailed mechanisms of how these specific initial
265 conditions could lead to block maintenance warrant further studies.

266

267

268 **Appendix A: A two-layer quasi-geostrophic model**

269 Following Wang and Lee (2016) (WL16), the two-layer QG model with an unequal layer
 270 thickness on a beta-plane:

$$\begin{aligned}
 271 \quad \frac{\partial q_1}{\partial t} + J(\psi_1, q_1) &= -\tau^{-1} \frac{\psi_2 - \psi_1 + \psi_R}{2(2-\delta)} - \kappa \nabla^6 \psi_1, \\
 \frac{\partial q_2}{\partial t} + J(\psi_2, q_2) &= \tau^{-1} \frac{\psi_2 - \psi_1 + \psi_R}{2\delta} - \gamma^{-1} \nabla^2 \psi_2 - \kappa \nabla^6 \psi_2,
 \end{aligned} \tag{A1}$$

272 where the quasi-geostrophic potential vorticity (PV) is:

$$\begin{aligned}
 273 \quad q_1 &= \beta y + \nabla^2 \psi_1 + \frac{\psi_2 - \psi_1}{2(2-\delta)}, \\
 q_2 &= \beta y + \nabla^2 \psi_2 - \frac{\psi_2 - \psi_1}{2\delta}.
 \end{aligned} \tag{A2}$$

274 The subscripts 1 and 2 refer to the upper and lower layers, respectively.

275 The nondimensional β measures the ratio of planetary vorticity gradient to vertical shear
 276 contribution. δ denotes nondimensional thickness of the lower layer at rest. The velocity field
 277 is determined by the relation $(u_i, v_i) = (-\partial\psi_i/\partial y, \partial\psi_i/\partial x)$. The time is non-dimensionalized by
 278 L_d/U , where horizontal length scale is $L_d = 750 \text{ km}$ and velocity scale is $U = 45 \text{ ms}^{-1}$. Hyper-
 279 viscosity is included in both layers to remove enstrophy at small scales. Ekman damping with a
 280 damping time scale γ of 1.5 day is included in the lower layer only, and thermal relaxation of
 281 the upper layer zonal mean flow to a prescribed jet-like ‘‘radiative equilibrium state’’

282 $U_e \equiv -\partial\psi_e/\partial y = \text{sech}^2(\frac{y}{2})$ and the lower layer to zero wind is adopted with a relaxation time
 283 scale of 30 days.

284 The equation (A1) is solved numerically with Fourier spectral decomposition in the zonal
 285 direction and sine function decomposition in the meridional direction. As in WL16, in this study
 286 we choose a layer thickness ratio of $\delta = 0.25$. The key findings in this study have been tested
 287 with other values (e.g. standard equal-layer thickness) and have been confirmed to be insensitive
 288 to the particular value of choice. The non-dimensional channel length and width are set to
 289 $L_x = 20\pi$ and $L_y = 5\pi$ respectively. The width chosen is sufficiently large so that eddy
 290 amplitude is eligible near the walls. A sponge layer is added at both northern and southern
 291 boundaries to avoid reflecting waves.

292

293

294 **Appendix B: A weakly nonlinear barotropic quasi-geostrophic model**

295 Following S83, we construct a similar weakly nonlinear barotropic QG model that is
 296 consistent with the above two-layer QG model.

297 Zero-order equation: the time-invariant mature block

$$298 \quad U_b \frac{\partial q_{b0}}{\partial x} + J(\psi_{b0}, q_{b0}) + \left(\beta - \frac{\partial^2 U_b}{\partial y^2}\right) \frac{\partial \psi_{b0}}{\partial x} = -D(\psi_{b0}) \quad (\text{B1})$$

299 First-order equation: incoming eddies and straining effects

$$300 \quad \left(\frac{\partial}{\partial t} + U_b \frac{\partial}{\partial x}\right) q_{b1} + J(\psi_{b1}, q_{b0}) + J(\psi_{b0}, q_{b1}) + \left(\beta - \frac{\partial^2 U_b}{\partial y^2}\right) \frac{\partial \psi_{b1}}{\partial x} = F_1 - D(\psi_{b1}) \quad (\text{B2})$$

301 Second-order equation: induced circulation

$$302 \quad \left(\frac{\partial}{\partial t} + U_b \frac{\partial}{\partial x}\right) q_{b2} + J(\psi_{b0}, q_{b2}) + J(\psi_{b2}, q_{b0}) + \left(\beta - \frac{\partial^2 U_b}{\partial y^2}\right) \frac{\partial \psi_{b2}}{\partial x} = -J(\psi_{b1}, q_{b1}) - D(\psi_{b2}) \quad (\text{B3})$$

303 where $U_b = \frac{2-\delta}{2}U_1 + \frac{\delta}{2}U_2$ denotes barotropic density-weighted zonal-mean zonal velocity.

304 q_{b0}, q_{b1}, q_{b2} denote zero-th order, first order, and second order of the barotropic PV with

305 $q_b = \frac{2-\delta}{2}q_1 + \frac{\delta}{2}q_2$, and similar notation is used for streamfunction $\psi_{b0}, \psi_{b1}, \psi_{b2}$.

306 A wave maker is prescribed by:

$$307 \quad F_1 = 1.0^{-12} \cdot \sin\left\{\frac{\pi(x-x_0)}{\Delta x}\right\} \cos\left\{\frac{3\pi(x-x_0-t)}{\Delta x}\right\} \exp\left\{-4\left(\frac{y-y_0}{\Delta y}\right)^2\right\} \quad (\text{B4})$$

308 where x_0 is the starting longitude of the wave maker, y_0 is the mid-point of the channel,

309 $\Delta x = L_x / 4$ and $\Delta y = L_y / 4$ are the zonal and meridional extent of the wave maker.

310

311 **Acknowledgments**

312 The authors acknowledge the computational resources at NCAR Yellowstone and Harvard
 313 Odyssey cluster. The authors acknowledge discussions with Dehai Luo, Akira Yamazaki,
 314 Pedram Hassanzadeh, and Brian Hoskins. This research was supported by NASA grant
 315 80NSSC17K0267, NSF grant AGS-1552385, and a grant from the Harvard Global Institute.

316

317 **References**

- 318 Arai, M., & Mukougawa, H. (2002). On the Effectiveness of the Eddy Straining Mechanism for
319 the Maintenance of Blocking Flows. *Journal of the Meteorological Society of Japan. Ser.*
320 *II*, 80(4B), 1089–1102. <https://doi.org/10.2151/jmsj.80.1089>
- 321 Barnes, E. A., Dunn□Sigouin, E., Masato, G., & Woollings, T. (2014). Exploring recent trends
322 in Northern Hemisphere blocking. *Geophysical Research Letters*, 41(2), 638–644.
323 <https://doi.org/10.1002/2013GL058745>
- 324 Berggren, R., Bolin, B., & Rossby, C.-G. (1949). An Aerological Study of Zonal Motion, its
325 Perturbations and Break-down. *Tellus*, 1(2), 14–37. [https://doi.org/10.1111/j.2153-](https://doi.org/10.1111/j.2153-3490.1949.tb01257.x)
326 [3490.1949.tb01257.x](https://doi.org/10.1111/j.2153-3490.1949.tb01257.x)
- 327 Haines, K., & Holland, A. J. (1998). Vacillation cycles and blocking in a channel. *Quarterly*
328 *Journal of the Royal Meteorological Society*, 124(547), 873–895.
329 <https://doi.org/10.1002/qj.49712454711>
- 330 Haines, Keith, & Marshall, J. (1987). Eddy-Forced Coherent Structures As A Prototype of
331 Atmospheric Blocking. *Quarterly Journal of the Royal Meteorological Society*, 113(476),
332 681–704. <https://doi.org/10.1002/qj.49711347613>
- 333 Holopainen, E., & Fortelius, C. (1987). High-Frequency Transient Eddies and Blocking. *Journal*
334 *of the Atmospheric Sciences*, 44(12), 1632–1645. [https://doi.org/10.1175/1520-](https://doi.org/10.1175/1520-0469(1987)044<1632:HFTEAB>2.0.CO;2)
335 [0469\(1987\)044<1632:HFTEAB>2.0.CO;2](https://doi.org/10.1175/1520-0469(1987)044<1632:HFTEAB>2.0.CO;2)
- 336 Hoskins, B. J., & James, I. N. (2014). *Fluid Dynamics of the Midlatitude Atmosphere* (Vol.
337 9780470833698). Chichester: John Wiley & Sons, Ltd.

- 338 Huang, C. S. Y., & Nakamura, N. (2016). Local Finite-Amplitude Wave Activity as a Diagnostic
339 of Anomalous Weather Events. *Journal of the Atmospheric Sciences*, 73(1), 211–229.
340 <https://doi.org/10.1175/JAS-D-15-0194.1>
- 341 Luo, D. (2000). Planetary-scale baroclinic envelope Rossby solitons in a two-layer model and
342 their interaction with synoptic-scale eddies. *Dynamics of Atmospheres and Oceans*,
343 32(1), 27–74. [https://doi.org/10.1016/S0377-0265\(99\)00018-4](https://doi.org/10.1016/S0377-0265(99)00018-4)
- 344 Luo, D. (2005). A Barotropic Envelope Rossby Soliton Model for Block–Eddy Interaction. Part
345 I: Effect of Topography. *Journal of the Atmospheric Sciences*, 62(1), 5–21.
346 <https://doi.org/10.1175/1186.1>
- 347 Maeda, S., Kobayashi, C., Takano, K., & Tsuyuki, T. (2000). Relationship between Singular
348 Modes of Blocking Flow and High-frequency Eddies. *Journal of the Meteorological
349 Society of Japan. Ser. II*, 78(5), 631–646. https://doi.org/10.2151/jmsj1965.78.5_631
- 350 Nakamura, N., & Huang, C. S. Y. (2018). Atmospheric blocking as a traffic jam in the jet stream.
351 *Science*, eaat0721. <https://doi.org/10.1126/science.aat0721>
- 352 Shutts, G. J. (1983). The propagation of eddies in diffluent jetstreams: Eddy vorticity forcing of
353 ‘blocking’ flow fields. *Quarterly Journal of the Royal Meteorological Society*, 109(462),
354 737–761. <https://doi.org/10.1002/qj.49710946204>
- 355 Vautard, R., Legras, B., & Déqué, M. (1988). On the Source of Midlatitude Low-Frequency
356 Variability. Part I: A Statistical Approach to Persistence. *Journal of the Atmospheric
357 Sciences*, 45(20), 2811–2844. [https://doi.org/10.1175/1520-
358 0469\(1988\)045<2811:OTSOML>2.0.CO;2](https://doi.org/10.1175/1520-0469(1988)045<2811:OTSOML>2.0.CO;2)
- 359 Wang, L., & Lee, S. (2016). The role of eddy diffusivity on poleward jet shift. *Journal of the
360 Atmospheric Sciences*. <https://doi.org/10.1175/JAS-D-16-0082.1>

361 Woollings, T., Barriopedro, D., Methven, J., Son, S.-W., Martius, O., Harvey, B., et al. (2018).

362 Blocking and its Response to Climate Change. *Current Climate Change Reports*, 4(3),

363 287–300. <https://doi.org/10.1007/s40641-018-0108-z>

364 Yamazaki, A., & Itoh, H. (2012). Vortex–Vortex Interactions for the Maintenance of Blocking.

365 Part I: The Selective Absorption Mechanism and a Case Study. *Journal of the*

366 *Atmospheric Sciences*, 70(3), 725–742. <https://doi.org/10.1175/JAS-D-11-0295.1>

367